Title: Goal-directed visual information processing with GABAergic inhibition in parietal cortex

Authors: Zhiyan Wang, Sinah Wiborg, Antonia Wittmann, Nina Beck, Markus Becker, Sebastian M. Frank

Affiliation: Institute for Experimental Psychology, University of Regensburg, 93053 Regensburg, Germany.

Correspondence: sebastian1.frank@psychologie.uni-regensburg.de

Funding: This research was supported by the Deutsche Forschungsgemeinschaft (DFG, German Research Foundation; Emmy Noether grant – project number 491290285), the Hector Fellow Academy, and the Julitta und Richard Müller Stiftung.

Declaration of Conflicting Interests: The author declares that there is no conflict of interest.

Abstract:

Goal-directed visual information processing involves tracking relevant visual signals (targets) over space and time. However, goal-irrelevant visual signals (distractors) can interfere with the tracking of targets. The neuronal mechanisms, which promote the tracking of targets in the challenge of interference from distractors remain elusive. Here, we used time-resolved functional magnetic resonance spectroscopy (fMRS) to measure dynamic changes of γ-aminobutyric acid (GABA), a chief inhibitory neurotransmitter, and glutamate, a chief excitatory neurotransmitter, in the parietal and visual cortices while participants performed a visual tracking task for targets among distractors. We found that the more targets had to be tracked, the greater the concentrations of GABA and glutamate in parietal cortex. In visual cortex only the concentration of glutamate increased with the number of tracking targets. Concentration changes of GABA and glutamate in parietal cortex only were differentially associated with performance: Better target tracking was associated with greater increase in GABA concentration and smaller increase in glutamate concentration. These results suggest that GABAergic inhibition in parietal cortex plays a crucial role in minimizing interference during target tracking over space and time, thereby promoting goal-directed visual information processing. (185 words)

Keywords: GABA, Glutamate, Goal-Directed Information Processing, Interference, Parietal Cortex, Tracking, Visual Cortex

Introduction

Tracking visual signals relevant to current goals across space and time is critical for adaptive behavior (Cavanagh & Alvarez, 2005; Chun et al., 2011; Egeth & Yantis, 1997; Scholl, 2001; Van Ede & Nobre, 2023; Xu & Chun, 2009). However, in a dynamically changing environment goal-irrelevant distractor signals compete for processing and can interfere with tracking of goal-relevant target signals. How is the interference between targets and distractors resolved? Previous results showed that there are distinct neural representations of targets and distractors in visual cortex (Christophel et al., 2012; Ester et al., 2013; Harrison & Tong, 2009; Rademaker et al., 2019; Serences, 2016; Sprague et al., 2014, 2015) and parietal cortex (Bracci et al., 2017; Buschman & Miller, 2007; Vaziri-Pashkam & Xu, 2017). Especially the representation of targets in parietal cortex was found to be robust against interference from distractors (Bettencourt & Xu, 2016; Lorenc et al., 2018; Xu, 2024). However, it is unclear which mechanisms promote the emergence of distinct target and distractor representation in parietal cortex.

Here, we investigated the hypothesis that GABAergic inhibition within parietal cortex may underlie a separation between target and distractor processing, thereby promoting the emergence of distinct target and distractor representations with minimal interference. GABA is a chief inhibitory neurotransmitter (Isaacson & Scanziani, 2011; Petroff, 2002; Schmidt-Wilcke et al., 2018; Tremblay et al., 2016; Tritsch et al., 2016) and critical for suppressing spontaneous activity related to distraction (Bang et al., 2018; De La Vega et al., 2014; Frangou et al., 2019; Frank et al., 2022; Shibata et al., 2017; H. R. Snyder et al., 2010; Tamaki et al., 2020; Yamada et al., 2024). While reduced GABAergic function can impair the selection of goal-relevant signals (H. R. Snyder et al., 2010), increased GABAergic activity is associated with enhanced efficiency in resolving competitions between task-relevant and task-irrelevant signals (De La Vega et al., 2014). On a cellular level, GABAergic inhibition minimizes interneuron correlations and promotes goal-relevant sensory signal processing (Cohen & Maunsell, 2009; Harris & Thiele, 2011; A. C. Snyder et al., 2016; Srivastava et al., 2023).

These results suggest that GABAergic inhibition may play a crucial role in separating goal-relevant target from goal-irrelevant distractor processing. If this is the case, an increase

in targets should lead to increased GABAergic inhibition to maintain a separation between target and distractor processing. To test this prediction, we used a recently advanced imaging method referred to as time-resolved functional magnetic resonance spectroscopy (fMRS) (Apšvalka et al., 2015; Craven et al., 2024; Lally et al., 2014; Stanley and Raz, 2018; Koolschijn et al., 2023; Mullins, 2018, 2024) to measure dynamic changes in the concentrations of GABA and glutamate in the parietal and visual cortices while participants performed a multiple object tracking (MOT) task (Cavanagh & Alvarez, 2005; Meyerhoff et al., 2017; Pylyshyn & Storm, 1988). In different conditions of MOT participants tracked two or four targets among multiple distractors, to manipulate the number of goal-relevant among goal-irrelevant visual signals (henceforth referred to as low and high load conditions). Importantly, the total number of visual stimuli (sum of targets and distractors) remained identical across conditions to maintain constant visual input (Alvarez & Franconeri, 2007; Cavanagh & Alvarez, 2005).

We found that GABA and glutamate concentrations in parietal cortex increased dynamically from the low to the high load condition. Critically, a greater increase of GABA concentration and lower increase of glutamate concentration in parietal cortex predicted better tracking performance in the high load condition. In visual cortex only the concentration of glutamate increased with load and no association with tracking performance was found. These results suggest a crucial role of GABAergic inhibition in parietal cortex for tracking visual target signals over space and time. By maintaining a sharp separation between target and distractor processing even under conditions of high load, GABA may promote the emergence of distinct target and distractor representations with minimal interference. This effect of GABA was only found in parietal but not in visual cortex, suggesting an important role of higher order areas for goal-directed visual information processing.

Methods

Participants

A combined total of 36 participants [26 females, 10 males, mean ± standard-error-of-the-mean (SEM) age = 24.2 ± 1.08 years old; 35 right-handed, one left-handed] with normal or corrected-to-normal vision was recruited. Participants gave informed written consent prior to participation. The study was approved by the internal review board of the University of Regensburg. Thirty participants completed fMRS-MEGAPRESS. A subset of twenty-four

participants also volunteered to complete fMRS-PRESS. Six additional new participants were recruited for fMRS-PRESS.

Attentional Tracking Task

A MOT task with two attentional load conditions (tracking two targets = low load; tracking four targets = high load) was used (Cavanagh & Alvarez, 2005; Meyerhoff et al., 2017; Pylyshyn & Storm, 1988) (Figure 1). Each trial consisted of cueing, tracking and response phases. The tracking phase was 12 s-long in each of fMRS-MEGAPRESS and fMRS-PRESS. The cueing and response phases were each 3 s-long for fMRS-MEGAPRESS and 2 s each for fMRS-PRESS. During the cueing phase a total of twelve disks (diameter: 0.5°) was arranged circularly on a black screen (24 x 18° in size). Disks remained stationary during the cueing phase. A subset of disks was highlighted in green as targets while the other disks (i.e., the distractors) were displayed in white. During the tracking phase, the highlighting was turned off and all disks moved independently with a speed of 4.5°/s in different and unpredictable directions across the screen. Each disk's motion trajectory was constrained to avoid collisions with other disks and overlap with the central fixation spot. Disks were repelled from the borders of the screen. For each trial and session trajectories were calculated in advance and randomly drawn (without replacement) from a predefined pool of unique trajectories that was used for each participant. Participants were instructed to track the targets with their attention and maintain central fixation. Each trial terminated with a response phase. During the response phase all disks remained stationary at their final position at the end of the tracking phase and one disk was highlighted in green. Participants indicated whether the highlighted disk was a target or a distractor by pressing one of two buttons on the MRI-safe buttonbox. In half of all trials, the highlighted disk was a target, resulting in a chance level of 50% correct response accuracy. Participants were instructed to respond as quickly and accurately as possible. No feedback about participants' response accuracy was provided.

Imaging Experiment

The imaging experiment included fMRS-MEGAPRESS and fMRS-PRESS runs. A checklist with all fMRS acquisition parameters, analyses and quality checks, as proposed by Choi et al., (2021), is provided in Table 1. In each fMRS run participants performed the attentional tracking task with low and high load conditions while a time-series of fMRS scans was collected (see Figure 1). Low and high load conditions were presented in random order within each fMRS run. For each load condition there was a total of 18 trials in fMRS-

MEGAPRESS and 9 trials in fMRS-PRESS. For fMRS a mixed design was used in which each trial with attentional tracking was followed by a jittered intertrial interval. This intertrial interval ranged between 9 s, 18 s, and 27 s in fMRS-MEGAPRESS and between 8 s, 16 s, and 24 s in fMRS-PRESS. During the intertrial interval a central fixation spot on an otherwise blank screen was displayed. The fMRS runs commenced and terminated with on-ramp and off-ramps, respectively, during which a central fixation spot on an otherwise blank screen was displayed. Ramps were 60 s long in fMRS-MEGAPRESS and 64 s long in fMRS-PRESS. Some studies reported that the concentration of GABA is modulated by the menstrual cycle (De Bondt et al., 2015; Duncan et al., 2014). Therefore, in female participants not using contraception, the imaging experiment was only conducted during the follicular phase.

Scanning Parameters

Single-voxel proton (^{1}H) fMRS was conducted for two types of fMRS scan (MEGAPRESS and PRESS, respectively) and volumes-of-interest (VOIs; located in the parietal and occipital lobes, respectively). MEGAPRESS scans (Mescher et al., 1996, 1998) were collected with alternating Edit On and Edit Off scans with the following scanning parameters: time-to-repeat (TR) = 1.5 s; time-to-echo (TE) = 68 ms; flip angle (FA) = 90°. The total number of scans (Edit On and Edit Off combined) was 472. A frequency selective, single band Gauss pulse was utilized to saturate the β-CH_2 signal at 1.94 ppm and to refocus the J evolution of the triplet γ-CH_2 resonance of GABA at 3 ppm ('Edit On'). The very same Gauss pulse was used to irradiate the opposite part of the spectrum at 7.46 ppm ('Edit Off'). The 'Edit Off' spectrum was subtracted from the 'Edit On' spectrum to produce a difference spectrum. For each load condition in fMRS-MEGAPRESS, there were a total of 18 scans for the cueing phase, 72 scans for the tracking phase, 18 scans for the response phase, 216 scans for the intertrial interval, and 20 scans for each ramp. The number of scans for the measurement of the concentration of GABA in each load condition followed the approach of previous studies (Floyer-Lea et al., 2006; Frank et al., 2022), which employed a minimum of 64 scans to estimated GABA from the MEGAPRESS difference spectrum. For PRESS (Bottomley et al., 1984; Bottomley & Hardy, 1987) the following scanning parameters were used: TR = 2 s; TE = 30 ms; FA = 90°; 352 scans in each fMRS-PRESS run. For each load condition in fMRS-PRESS, there were a total of 9 scans for the cueing phase, 54 scans for the tracking phase, 9 scans for the response phase, 144 scans for the intertrial interval, and 32 scans for each ramp.

WET water suppression was used (Ogg et al., 1994). There was a total of four fMRS runs for each VOI and type of fMRS scan (i.e., fMRS-MEGAPRESS for parietal VOI, fMRS-MEGAPRESS for visual VOI, fMRS-PRESS for parietal VOI, and fMRS-PRESS for visual VOI). The parietal VOI had a size of 2 x 2 x 4 cm and was placed approximately perpendicular to the intraparietal sulcus. The visual VOI had a size of 2 x 2 x 2 cm and was placed perpendicular to the calcarine sulcus. Proximity to the dura was avoided during VOI placement to minimize macromolecule contamination. See Figure 2 for VOI locations in a representative participant. VOIs were centered between the two hemispheres. Non-neural tissue containing lipids was avoided during VOI placement. For the purpose of VOI placement, three short high-resolution anatomical scans were collected for the coronal, sagittal and transverse planes prior to fMRS. These anatomical scans had the following scanning parameters: coronal plane: TR = 0.25 s, TE = 2.46 ms, FA = 70°, acquisition matrix (AM) = 288 x 288, 35 slices, voxel size = 0.8 x 0.8 x 4.0 mm, inter-slice gap = 1.20 mm; sagittal plane: TR = 0.19 s, TE = 2.46 ms, FA = 70°, AM = 288 x 288, 25 slices, voxel size = 0.8 x 0.8 x 4.0 mm, inter-slice gap = 1.20 mm; transverse plane: TR = 0.19 s, TE = 2.46 ms, FA = 70°, AM = 288 x 288, 27 slices, voxel size = 0.8 x 0.8 x 4.0 mm, inter-slice gap = 1.20 mm. For each VOI water reference scans without water suppression were collected after each fMRS run with the following scanning parameters: fMRS-MEGAPRESS: TR = 1.5 s; TE = 30 ms; FA = 90°; 8 scans; fMRS-PRESS: TR = 2 s; TE = 30 ms; FA = 90°; 16 scans.

Automatic shimming (gradient field adjustments to increase the homogeneity of the magnet field B_0) was conducted prior to each fMRS run. For each fMRS run and participant the shim values were kept below a full-width at half-maximum (FWHM) of 20 Hz. The mean ± SEM shim values across participants were as follows: fMRS-MEGAPRESS: 13.6 ± 0.26 Hz (parietal VOI) and 13.8 ± 0.18 Hz (visual VOI); fMRS-PRESS: 13.6 ± 0.22 Hz (parietal VOI) and 14.5 ± 0.26 Hz (visual VOI); water reference scan in fMRS-MEGAPRESS: 13.9 ± 0.31 Hz (parietal VOI) and 13.9 ± 0.21 Hz (visual VOI); water reference scan in fMRS-PRESS: 13.7 ± 0.28 Hz (parietal VOI) and 14.5 ± 0.24 Hz (visual VOI).

In order to calculate volume fractions for each VOI (see *Imaging Analysis* below) we also collected a high-resolution anatomical scan of the brain using a magnetization prepared rapid gradient echo sequence with the following scanning parameters: TR= 2.3 s, TE = 2.32 ms, FA = 8°, AM = 256 x 256, 192 sagittal slices, voxel size = 0.9 x 0.9 x 0.9 mm, interslice gap = 0.45 mm.

Stimulus Presentation

Stimuli were generated using Psychtoolbox (Brainard, 1997; Pelli, 1997) running in Matlab (The Mathworks, Natick, MA, USA). Stimuli were presented using a projector with gamma-correction onto a translucent screen located at the back of the scanner bore. Participants viewed the screen with a headcoil-mounted mirror.

Behavioral Analysis

Response accuracy and median response time (in seconds) were combined into the inverse efficiency score for each fMRS run and participant (Townsend & Ashby, 1978, 1983). To this purpose median response time was divided by response accuracy (in proportion of one) and the result was log-transformed (Bruyer & Brysbaert, 2011). For one participant, the response accuracy was at chance level in fMRS-MEGAPRESS. The behavioral and fMRS-MEGAPRESS results from this participant were excluded from all further analyses.

Imaging Analysis

fMRS data were analyzed using the LC Model (Provencher, 1993, 2001). An analysis protocol as in previous studies was applied (Frank et al., 2023). Details are reported in Table 1 (Choi et al., 2021; Lin et al., 2021). Before running the analysis, spectra from different scans in the fMRS time-series were averaged across trials and conditions as follows. Average spectra were produced for the tracking phase in each load condition for trials with correct participant response (Supplementary Figures 1, 2). The mean ± SEM number of spectra used for averaging across participants were as follows: fMRS-MEGAPRESS: 69.7 ± 0.81 (parietal VOI) and 70.5 ± 0.46 (visual VOI) in the low load condition; 63.3 ± 1.45 (parietal VOI) and 61.7 ± 1.58 (visual VOI) in the high load condition; fMRS-PRESS: 50.0 ± 1.01 (parietal VOI) and 51.4 ± 0.80 (visual VOI) in the low load condition; 47.8 ± 1.33 (parietal VOI) and 48.2 ± 0.97 (visual VOI) in the high load condition.

The averaged MEGAPRESS difference scans were analyzed in the chemical shift range between 1.95 and 4.2 ppm. The averaged PRESS scans were analyzed in the chemical shift range between 0.2 and 4.0 ppm. Water scaling and eddy current correction were performed. The metabolite intensities were fitted to a linear combination of spectra of individual metabolites derived from an imported metabolite basis set (Provencher, 1993, 2001:Table 1).

The following metabolite concentrations estimated for the tracking phase of each load condition in each fMRS run were further analyzed: fMRS-MEGAPRESS: GABA and N-acetyl-aspartate (NAA). NAA is a marker of neuronal density and mitochondrial function

(Schuff et al., 2006) and is commonly used as a control metabolite to normalize the concentrations of GABA and Glx (Duncan et al., 2014; Frank et al., 2023; Mullins et al., 2014; Stagg, 2014). fMRS-PRESS: Glx (corresponding to the composite measure of glutamate and its precursor glutamine) and NAA. Before normalization GABA, Glx, and NAA concentrations were corrected for each participant's volume fractions inside the fMRS VOIs. Volume fractions within the fMRS VOIs corresponding to gray matter, white matter and other types of volume including cerebrospinal fluid were calculated using the Freesurfer segmentation of each participant's reconstructed high-resolution anatomical scan of the brain (Dale et al., 1999; Fischl et al., 1999; Martinos Center for Biomedical Imaging, Charlestown, MA, USA). Across participants the mean ± SEM volume fractions were as follows: Gray matter: 60.9 ± 1.11% (parietal VOI) and 60.1 ± 0.90% (visual VOI); white matter: 14.8 ± 0.64% (parietal VOI) and 34.1 ± 0.89% (visual VOI); other types of volume: 24.4 ± 1.25% (parietal VOI) and 5.85 ± 0.59% (visual VOI). Volume correction was performed using the approach proposed Kolasinski et al., (2017). The concentrations of GABA and Glx were corrected for the proportion of gray matter within each VOI by dividing by [gray matter / (gray matter + white matter + other)]. The concentration of NAA was corrected for the proportion of total brain volume within each VOI by dividing by [(gray matter + white matter) / (gray matter + white matter + other)]. Thereafter, for fMRS-MEGAPRESS the corrected concentration of GABA was normalized by dividing it by the corrected concentration of NAA extracted from the same MEGAPRESS difference spectrum. For fMRS-PRESS the corrected concentration of Glx was normalized by dividing it by the corrected concentration of NAA extracted from the same PRESS spectrum.

Post-hoc analyses were performed to calculate which anatomical brain regions were included within the gray matter in each VOI. The PALS segmentation (Van Essen, 2005) was remapped from the Freesurfer standard brain to each participant's individual brain and the percentage of Brodmann areas with the gray matter of each VOI was calculated for each participant. Across participants, seventy percent of gray matter within the parietal VOI corresponded to Brodmann areas 1, 2, 3, 5, 7 and 31 (areas 1-3: 7.69 ± 0.90%; area 5: 23.2 ± 1.24%; area 7: 21.1 ± 1.27%; area 31: 18.1 ± 1.54%). The remaining gray matter corresponded mostly to the medial part of Brodmann area 4 (28.3 ± 2.39%). Within the gray matter of the visual VOI 60.4 ± 2.10% corresponded to Brodmann area 17 and 37.5 ± 1.95% corresponded to Brodmann area 18 across participants. Gray matter corresponding to other areas was negligible. The mean ± SEM MNI coordinates of the parietal and visual VOIs

across participants were as follows: Parietal VOI: X = -0.14 ± 0.23, Y = -49.3 ± 0.76, Z = 52.1 ± 0.64; Visual VOI: X = 0.39 ± 0.31, Y = -81.4 ± 0.42, Z = 4.39 ± 0.54.

We only included spectral results for which the signal-to-noise (SN) ratio as estimated by the LC model was higher than 5% (see Wilson et al., 2019). None of a participant's spectra had to be excluded. The mean SN% (± SEM) across participants' spectra was as follows: fMRS-MEGAPRESS: 24.8 ± 1.42% (parietal VOI) and 16.2 ± 0.54% (visual VOI) in the low load condition; 23.1 ± 1.14% (parietal VOI) and 15.2 ± 0.51% (visual VOI) in the high load condition; fMRS-PRESS: 30.2 ± 1.36% (parietal VOI) and 28.7 ± 0.83% (visual VOI) in the low load condition; 29.7 ± 1.39% (parietal VOI) and 28.1 ± 0.85% (visual VOI) in the high load condition.

The Cramer-Rao Lower Bounds (CRLB) indicate the reliability of quantification of GABA, Glx, and NAA. A criterion of 25% was used to reject low-quality results (following the approach in Frank et al., 2022) Using this criterion, the results for fMRS-MEGAPRESS were as follows: Parietal VOI: For two participants GABA results from the low load condition and for one participant GABA results from the low and high load conditions were above the CRLB inclusion criterion. Visual VOI: For two participants GABA results from the low load condition and for another two participants GABA results from the high load condition were above the CRLB inclusion criterion. GABA and NAA results from these participants were excluded. Therefore, out of 29 participants in fMRS-MEGAPRESS, GABA and NAA results in each load condition for 26 participants in the parietal VOI and for 25 participants in the visual VOI were further analyzed. None of the Glx and NAA results in any condition and VOI in fMRS-PRESS exceeded the CRLB inclusion criterion. The mean CRLB% (± SEM) across included participants were as follows: GABA in fMRS-MEGAPRESS: 16.8 ± 0.58% (parietal VOI) and 19.4 ± 0.57% (visual VOI) in the low load condition; 15.4 ± 0.42% (parietal VOI) and 20.1 ± 0.49% (visual VOI) in the high load condition; NAA in fMRS-MEGAPRESS: 3.50 ± 0.16% (parietal VOI) and 3.40 ± 0.10% (visual VOI) in the low load condition; 3.69 ± 0.15% (parietal VOI) and 3.72 ± 0.12% (visual VOI) in the high load condition; Glx in fMRS-PRESS: 6.47 ± 0.15% (parietal VOI) and 6.73 ± 0.17% (visual VOI) in the low load condition; 6.10 ± 0.14% (parietal VOI) and 6.70 ± 0.13% (visual VOI) in the high load condition; NAA in fMRS-PRESS: 2.60 ± 0.10% (parietal VOI) and 2.57 ± 0.11% (visual VOI) in the low load condition; 2.67 ± 0.11% (parietal VOI) and 2.70 ± 0.11% (visual VOI) in the high load condition.

Statistics

The results were analyzed using *t*-tests and Pearson correlations. The two-tailed alpha-level was set to 0.05. Cohen's *d*, and Pearson's *r* were calculated as measures of effect size for *t*-test and Pearson correlation, respectively. Cohen's *d* for repeated measures was calculated using the formula implemented in G*Power (Faul et al., 2007).

Results

The behavioral results showed that the inverse efficiency score was significantly greater in the high than the low load condition [$t(34) = 5.79$, $p < 0.001$, $d = 0.98$], indicating that participants responded slower and were less accurate in tracking with high than low load (see Supplementary Figure 3).

The fMRS-MEGAPRESS results showed that the concentration of GABA was significantly greater in the high than the low load condition in the parietal VOI [$t(25) = 3.25$, $p = 0.003$, $d = 0.64$] but not in the visual VOI [$t(24) = -0.84$, $p = 0.41$] (Figure 2). The concentration of the control metabolite NAA was not significantly different between the low and high load conditions in any VOI [parietal VOI: $t(25) = 0.02$, $p = 0.99$; visual VOI: $t(24) = -0.81$, $p = 0.43$] (Supplementary Figure 4).

The fMRS-PRESS results showed that the concentration of Glx was significantly greater in the high than the low load condition in the parietal VOI [$t(29) = 3.27$, $p = 0.003$, $d = 0.60$] and the visual VOI [$t(29) = 2.37$, $p = 0.02$, $d = 0.43$] (Figure 2). The concentration of the control metabolite NAA was not significantly different between the low and high load conditions in any VOI [parietal VOI: $t(29) = 0.64$, $p = 0.53$; visual VOI: $t(29) = -0.37$, $p = 0.71$] (Supplementary Figure 4).

The fMRS and behavioral results in the parietal VOI were correlated (Figure 3). The greater was the increase of GABA from the low to the high load condition, the smaller was the difference in inverse efficiency score between the two load conditions (the smaller was the decrease in response accuracy and increase in response time from low to high load) across participants ($r = -0.47$, $p = 0.02$). There was no significant association in the visual VOI ($r = -0.17$, $p = 0.43$). A different association was found between Glx and behavioral changes with load: The greater the increase of Glx from the low to the high load condition, the greater was the increase in inverse efficiency score with load (i.e., the worse was response accuracy and the slower was response time in high than low load) across participants ($r = 0.49$, $p = 0.006$). There was no significant association in the visual VOI ($r = 0.24$, $p = 0.21$).

Discussion

We examined how visual signals relevant to current goals can be processed while being interfered with by goal-irrelevant distractor signals. For this purpose, we used a MOT task in which participants tracked goal-relevant target objects among goal-irrelevant distractor objects. In order to identify the neuronal mechanisms involved in minimizing interference between target and distractor processing, the number of targets was varied between tracking conditions with low and high load (corresponding to tracking two and four targets among distractors, respectively). We used fMRS to measure dynamic changes in inhibitory (GABAergic) and excitatory (glutamatergic) processing between tracking with low and high load. fMRS measurements were carried out in two brain regions relevant for goal-directed visual information processing (parietal and visual cortex, respectively). Our results showed that GABA and Glx concentrations both increased in parietal cortex during tracking with high load compared to tracking with low load. In visual cortex only the concentration of Glx increased with load. Correlational analyses showed that greater increases in GABA concentration and greater decreases in Glx concentration were associated with better tracking performance with increasing load across participants.

Our results suggest a key role of GABAergic inhibition for goal-directed visual information processing. GABA is a chief inhibitory neurotransmitter involved in refining neuronal responses for goal-relevant signals (De La Vega et al., 2014; Isaacson & Scanziani, 2011; Koolschijn et al., 2019; Okun & Lampl, 2008; Schmidt-Wilcke et al., 2018; H. R. Snyder et al., 2010; Tremblay et al., 2016; Tritsch et al., 2016; Wehr & Zador, 2003). The increase in GABA concentration with load may indicate that competition from spontaneous signals evoked by distractors is suppressed, leading to refined processing of goal-relevant information. This is comparable to findings observed with other types of cognitive tasks including semantic memory and selection during language processing, which showed that increased levels of GABA sharpened the representation of relevant information for a more efficient and precise selection among competitive semantic or linguistic information (De La Vega et al., 2014; Koolschijn et al., 2019; Williams et al., 2023). It is possible that increased levels of GABA reflect a general mechanism underlying the brain's ability to resist interference from irrelevant and unwanted signals and is universally used as a mechanism in different types of cognitive tasks (Isaacson & Scanziani, 2011; Tremblay et al., 2016; Tritsch et al., 2016). The increase in GABA concentration with load only in parietal cortex is consistent with previous results from functional magnetic resonance imaging (fMRI) showing that the representation of goal-relevant information in parietal cortex rather than visual cortex

is resilient to interference from goal-irrelevant signals (Bettencourt & Xu, 2016; Lorenc et al., 2018; Xu, 2024).

The increase in glutamate concentration in visual and parietal cortex with load may reflect target enhancement at early and late stages of visual processing. Studies using electroencephalographic recordings during MOT found increased stimulus-evoked potentials for targets compared with distractors in (early) visual cortex (Adamian & Andersen, 2022; Störmer et al., 2013, 2014), suggesting that target enhancement already occurs at early stages of cortical visual processing. Studies using fMRI showed that the blood-oxygenation-level-dependent (BOLD) response during MOT increased with the number of targets being tracked in parietal cortex (Alnaes et al., 2014; Culham et al., 1998; Frank et al., 2016; Jahn et al., 2012; Jovicich et al., 2001; Nummenmaa et al., 2017; Shim et al., 2010). This increase of BOLD in parietal cortex with load may reflect activation in gain maps, which highlight the locations of targets during MOT (Cavanagh et al., 2023). It is possible that increased BOLD activation in parietal gain maps may reflect a combination of both excitatory and inhibitory processing. Evidence from animal models (Isaacson & Scanziani, 2011; Okun & Lampl, 2008; Wehr & Zador, 2003), humans (Koolschijn et al., 2019) as well as computational research (Carandini & Heeger, 2012) showed that concurrent changes of excitatory and inhibitory input sharpen neuronal responses. A concurrent increase in excitatory and inhibitory processing, as observed in this study, would result in a sharp separation between target and distractor representations in parietal gain maps through glutamatergic enhancement of targets and GABAergic suppression of interfering distractor activity.

Our results also showed that changes in glutamate and GABA concentrations with load were differentially related to performance in MOT. Higher performance in MOT with increasing load was associated with greater glutamate decrease and greater GABA increase across participants. This suggests that target enhancement with glutamatergic processing may be most necessary when the task proves challenging to participants, whereas high-performing participants engage GABAergic processing to a greater extent to minimize interference between target and distractors.

Using fMRI, it is difficult to separate the contributions of excitatory and inhibitory processing to the hemodynamic response. Therefore, it is uncertain whether increased BOLD responses with load during MOT reflect increased excitatory or inhibitory activity or a combination of both. fMRS is a novel imaging approach that overcomes this limitation of fMRI (Apšvalka et al., 2015; Craven et al., 2024; Koolschijn et al., 2023; Lally et al., 2014; Mullins, 2018, 2024; Stanley & Raz, 2018). In addition, with fMRS it is possible to detect

glutamate and GABA changes with little delay compared to fMRI (Mullins, 2018). However, fMRS also has limitations that should be considered when interpreting the results of this study. Due to the large VOI size required for fMRS, the measured concentrations reflect a combination of extracellular and intracellular neurotransmitter concentrations across large portions of the parietal and occipital lobes. Although previous studies found extended activations in the parietal and visual cortex during MOT (Adamian & Andersen, 2022; Alnaes et al., 2014; Culham et al., 2001; Frank et al., 2016; Jahn et al., 2012; Jovicich et al., 2001; Nummenmaa et al., 2017; Shim et al., 2010; Störmer et al., 2013, 2014), possible differences between subregions or the precise localization of excitatory and inhibitory neural populations in gain maps cannot be measured with fMRS. The time-resolved fMRS design used in this study make it likely that the concentration changes result from neurotransmission rather than slower metabolic processes related to glutamate and GABA production. However, it is still possible that both processes contributed to the measured concentration changes.

In conclusion, the results of this study suggest that GABAergic inhibition is crucial for goal-directed visual information processing. By minimizing interference between target and distractor signals, GABAergic inhibition promotes the emergence of distinct goal-relevant and goal-irrelevant representations in parietal cortex. With such sharply separate representations, visual target signals can be tracked over space and time with minimal interference from distraction.

Author Contribution: Z.W. and S.M.F. designed the study. Z.W., S.W., A.W., N.B., M.B., and S.M.F. collected data. Z.W. and S.M.F. analyzed data. Z.W. and S.M.F. interpreted results. Z.W. and S.M.F. wrote the first draft of the manuscript. Z.W., M.B., and S.M.F. edited and revised manuscript. S.M.F. approved final version of manuscript. S.M.F. acquired funding.

References

Adamian, N., & Andersen, S. K. (2022). Attentional Enhancement of Tracked Stimuli in Early Visual Cortex Has Limited Capacity. *The Journal of Neuroscience: The Official Journal of the Society for Neuroscience*, *42*(46), 8709–8715. https://doi.org/10.1523/JNEUROSCI.0605-22.2022

Alnaes, D., Sneve, M. H., Espeseth, T., Endestad, T., Van De Pavert, S. H. P., & Laeng, B. (2014). Pupil size signals mental effort deployed during multiple object tracking and predicts brain activity in the dorsal attention network and the locus coeruleus. *Journal of Vision*, *14*(4), 1–1. https://doi.org/10.1167/14.4.1

Alvarez, G. A., & Franconeri, S. L. (2007). How many objects can you track?: Evidence for a resource-limited attentive tracking mechanism. *Journal of Vision*, *7*(13), 14. https://doi.org/10.1167/7.13.14

Apšvalka, D., Gadie, A., Clemence, M., & Mullins, P. G. (2015). Event-related dynamics of glutamate and BOLD effects measured using functional magnetic resonance spectroscopy (fMRS) at 3T in a repetition suppression paradigm. *NeuroImage*, *118*, 292–300. https://doi.org/10.1016/j.neuroimage.2015.06.015

Bang, J. W., Shibata, K., Frank, S. M., Walsh, E. G., Greenlee, M. W., Watanabe, T., & Sasaki, Y. (2018). Consolidation and reconsolidation share behavioural and neurochemical mechanisms. *Nature Human Behaviour*, *2*(7), 507–513. https://doi.org/10.1038/s41562-018-0366-8

Bettencourt, K. C., & Xu, Y. (2016). Decoding the content of visual short-term memory under distraction in occipital and parietal areas. *Nature Neuroscience*, *19*(1), 150–157. https://doi.org/10.1038/nn.4174

Bottomley, P. A., Foster, T. B., & Darrow, R. D. (1984). Depth-resolved surface-coil spectroscopy (DRESS) for in Vivo 1H, 31P, and 13C NMR. *Journal of Magnetic Resonance (1969)*, *59*(2), 338–342. https://doi.org/10.1016/0022-2364(84)90179-3

Bottomley, P. A., & Hardy, C. J. (1987). PROGRESS in efficient three-dimensional spatially localized in vivo31P NMR spectroscopy using multidimensional spatially selective (ϱ) pulses. *Journal of Magnetic Resonance (1969)*, *74*(3), 550–556. https://doi.org/10.1016/0022-2364(87)90276-9

Bracci, S., Daniels, N., & Op de Beeck, H. (2017). Task Context Overrules Object- and Category-Related Representational Content in the Human Parietal Cortex. *Cerebral Cortex (New York, N.Y.: 1991)*, *27*(1), 310–321. https://doi.org/10.1093/cercor/bhw419

Brainard, D. H. (1997). The Psychophysics Toolbox. *Spatial Vision*, *10*(4), 433–436.

Bruyer, R., & Brysbaert, M. (2011). Combining Speed and Accuracy in Cognitive Psychology: Is the Inverse Efficiency Score (IES) a Better Dependent Variable than the Mean Reaction Time (RT) and the Percentage Of Errors (PE)? *Psychologica Belgica*, *51*(1), 5. https://doi.org/10.5334/pb-51-1-5

Buschman, T. J., & Miller, E. K. (2007). Top-Down Versus Bottom-up Control of Attention in the Prefrontal and Posterior Parietal Cortices. *Science*, *315*(Ci), 1860–1862. https://doi.org/10.1126/science.1138071

Carandini, M., & Heeger, D. (2012). Normalization as a canonical neural computation. *Nature Reviews Neuroscience*, *November*, 1–12. https://doi.org/10.1038/nrn3136

Cavanagh, P., & Alvarez, G. (2005). Tracking multiple targets with multifocal attention. *Trends in Cognitive Sciences*, *9*(7), 349–354. https://doi.org/10.1016/j.tics.2005.05.009

Cavanagh, P., Caplovitz, G. P., Lytchenko, T. K., Maechler, M. R., Tse, P. U., & Sheinberg, D. L. (2023). The Architecture of Object-Based Attention. *Psychonomic Bulletin & Review*, *30*(5), 1643–1667. https://doi.org/10.3758/s13423-023-02281-7

Choi, I., Andronesi, O. C., Barker, P., Bogner, W., Edden, R. A. E., Kaiser, L. G., Lee, P., Marjańska, M., Terpstra, M., & De Graaf, R. A. (2021). Spectral editing in^{1} H magnetic resonance spectroscopy: Experts' consensus recommendations. *NMR in Biomedicine*, *34*(5), e4411. https://doi.org/10.1002/nbm.4411

Christophel, T. B., Hebart, M. N., & Haynes, J.-D. (2012). Decoding the Contents of Visual Short-Term Memory from Human Visual and Parietal Cortex. *The Journal of Neuroscience*, *32*(38), 12983–12989. https://doi.org/10.1523/JNEUROSCI.0184-12.2012

Chun, M. M., Golomb, J. D., & Turk-Browne, N. B. (2011). A Taxonomy of External and Internal Attention. *Annual Review of Psychology*, *62*(1), 73–101. https://doi.org/10.1146/annurev.psych.093008.100427

Cohen, M. R., & Maunsell, J. H. R. (2009). Attention improves performance primarily by reducing interneuronal correlations. *Nature Neuroscience*, *12*(12), 1594–1600. https://doi.org/10.1038/nn.2439

Craven, A. R., Dwyer, G., Ersland, L., Kazimierczak, K., Noeske, R., Sandøy, L. B., Johnsen, E., & Hugdahl, K. (2024). GABA, glutamatergic dynamics and BOLD contrast assessed concurrently using functional MRS during a cognitive task. *NMR in Biomedicine*, *37*(3), e5065. https://doi.org/10.1002/nbm.5065

Culham, J. C., Brandt, S. A., Cavanagh, P., Kanwisher, N. G., Dale, A. M., & Tootell, R. B. H. (1998). Cortical fMRI Activation Produced by Attentive Tracking of Moving Targets. *Journal of Neurophysiology*, *80*(5), 2657–2670. https://doi.org/10.1152/jn.1998.80.5.2657

Culham, J. C., Cavanagh, P., & Kanwisher, N. G. (2001). Attention Response Functions. *Neuron*, *32*(4), 737–745. https://doi.org/10.1016/S0896-6273(01)00499-8

Dale, A. M., Fischl, B., & Sereno, M. I. (1999). Cortical surface-based analysis. I. Segmentation and surface reconstruction. *NeuroImage*, *9*(2), 179–194. https://doi.org/10.1006/nimg.1998.0395

De Bondt, T., De Belder, F., Vanhevel, F., Jacquemyn, Y., & Parizel, P. M. (2015). Prefrontal GABA concentration changes in women-Influence of menstrual cycle phase, hormonal contraceptive use, and correlation with premenstrual symptoms. *Brain Research*, *1597*, 129–138. https://doi.org/10.1016/j.brainres.2014.11.051

De La Vega, A., Brown, M. S., Snyder, H. R., Singel, D., Munakata, Y., & Banich, M. T. (2014). Individual Differences in the Balance of GABA to Glutamate in pFC Predict the Ability to Select among Competing Options. *Journal of Cognitive Neuroscience*, *26*(11), 2490–2502. https://doi.org/10.1162/jocn_a_00655

Duncan, N. W., Wiebking, C., & Northoff, G. (2014). Associations of regional GABA and glutamate with intrinsic and extrinsic neural activity in humans—A review of multimodal imaging studies. *Neuroscience & Biobehavioral Reviews*, *47*, 36–52. https://doi.org/10.1016/j.neubiorev.2014.07.016

Egeth, H. E., & Yantis, S. (1997). VISUAL ATTENTION: Control, Representation, and Time Course. *Annual Review of Psychology*, *48*(1), 269–297. https://doi.org/10.1146/annurev.psych.48.1.269

Ester, E. F., Anderson, D. E., Serences, J. T., & Awh, E. (2013). A Neural Measure of Precision in Visual Working Memory. *Journal of Cognitive Neuroscience*, *25*(5), 754–761. https://doi.org/10.1162/jocn_a_00357

Faul, F., Erdfelder, E., Lang, A.-G., & Buchner, A. (2007). G*Power 3: A flexible statistical power analysis program for the social, behavioral, and biomedical sciences. *Behavior Research Methods*, *39*(2), 175–191. https://doi.org/10.3758/BF03193146

Fischl, B., Sereno, M. I., & Dale, A. M. (1999). Cortical surface-based analysis. II: Inflation, flattening, and a surface-based coordinate system. *NeuroImage*, *9*(2), 195–207. https://doi.org/10.1006/nimg.1998.0396

Floyer-Lea, A., Wylezinska, M., Kincses, T., & Matthews, P. M. (2006). Rapid modulation of GABA concentration in human sensorimotor cortex during motor learning. *Journal of Neurophysiology*, *95*(3), 1639–1644. https://doi.org/10.1152/jn.00346.2005

Frangou, P., Emir, U. E., Karlaftis, V. M., Nettekoven, C., Hinson, E. L., Larcombe, S., Bridge, H., Stagg, C. J., & Kourtzi, Z. (2019). Learning to optimize perceptual decisions through suppressive interactions in the human brain. *Nature Communications*, *10*(1), 474. https://doi.org/10.1038/s41467-019-08313-y

Frank, S. M., Becker, M., Malloni, W. M., Sasaki, Y., Greenlee, M. W., & Watanabe, T. (2023). Protocol to conduct functional magnetic resonance spectroscopy in different age groups of human participants. *STAR Protocols*, *4*(3), 102493. https://doi.org/10.1016/j.xpro.2023.102493

Frank, S. M., Becker, M., Qi, A., Geiger, P., Frank, U. I., Rosedahl, L. A., Malloni, W. M., Sasaki, Y., Greenlee, M. W., & Watanabe, T. (2022). Efficient learning in children with rapid GABA boosting during and after training. *Current Biology: CB*, *32*(23), 5022-5030.e7. https://doi.org/10.1016/j.cub.2022.10.021

Frank, S. M., Sun, L., Forster, L., Tse, P. U., & Greenlee, M. W. (2016). Cross-Modal Attention Effects in the Vestibular Cortex during Attentive Tracking of Moving Objects. *The Journal of Neuroscience: The Official Journal of the Society for Neuroscience*, *36*(50), 12720–12728. https://doi.org/10.1523/JNEUROSCI.2480-16.2016

Harris, K. D., & Thiele, A. (2011). Cortical state and attention. *Nature Reviews Neuroscience*, *12*(9), 509–523. https://doi.org/10.1038/nrn3084

Harrison, S. A., & Tong, F. (2009). Decoding reveals the contents of visual working memory in early visual areas. *Nature*, *458*(7238), 632–635. https://doi.org/10.1038/nature07832

Isaacson, J. S., & Scanziani, M. (2011). How inhibition shapes cortical activity. *Neuron*, *72*(2), 231–243. https://doi.org/10.1016/j.neuron.2011.09.027

Jahn, G., Wendt, J., Lotze, M., Papenmeier, F., & Huff, M. (2012). Brain activation during spatial updating and attentive tracking of moving targets. *Brain and Cognition*, *78*(2), 105–113. https://doi.org/10.1016/j.bandc.2011.12.001

Jovicich, J., Peters, R. J., Koch, C., Braun, J., Chang, L., & Ernst, T. (2001). Brain Areas Specific for Attentional Load in a Motion-Tracking Task. *Journal of Cognitive Neuroscience*, *13*(8), 1048–1058. https://doi.org/10.1162/089892901753294347

Kolasinski, J., Logan, J. P., Hinson, E. L., Manners, D., Divanbeighi Zand, A. P., Makin, T. R., Emir, U. E., & Stagg, C. J. (2017). A Mechanistic Link from GABA to Cortical Architecture and Perception. *Current Biology: CB*, *27*(11), 1685-1691.e3. https://doi.org/10.1016/j.cub.2017.04.055

Koolschijn, R. S., Clarke, W. T., Ip, I. B., Emir, U. E., & Barron, H. C. (2023). Event-related functional magnetic resonance spectroscopy. *NeuroImage*, *276*, 120194. https://doi.org/10.1016/j.neuroimage.2023.120194

Koolschijn, R. S., Emir, U. E., Pantelides, A. C., Nili, H., Behrens, T. E. J., & Barron, H. C. (2019). The Hippocampus and Neocortical Inhibitory Engrams Protect against Memory Interference. *Neuron*, *101*(3), 528-541.e6. https://doi.org/10.1016/j.neuron.2018.11.042

Lally, N., Mullins, P. G., Roberts, M. V., Price, D., Gruber, T., & Haenschel, C. (2014). Glutamatergic correlates of gamma-band oscillatory activity during cognition: A concurrent ER-MRS and EEG study. *NeuroImage*, *85 Pt 2*, 823–833. https://doi.org/10.1016/j.neuroimage.2013.07.049

Lin, A., Andronesi, O., Bogner, W., Choi, I.-Y., Coello, E., Cudalbu, C., Juchem, C., Kemp, G. J., Kreis, R., Krššák, M., Lee, P., Maudsley, A. A., Meyerspeer, M., Mlynarik, V., Near, J., Öz, G., Peek, A. L., Puts, N. A., Ratai, E.-M., … Experts' Working Group on Reporting Standards for MR Spectroscopy. (2021). Minimum Reporting Standards for in vivo Magnetic Resonance Spectroscopy (MRSinMRS): Experts' consensus recommendations. *NMR in Biomedicine*, *34*(5), e4484. https://doi.org/10.1002/nbm.4484

Lorenc, E. S., Sreenivasan, K. K., Nee, D. E., Vandenbroucke, A. R. E., & D'Esposito, M. (2018). Flexible Coding of Visual Working Memory Representations during Distraction. *The Journal of Neuroscience*, *38*(23), 5267–5276. https://doi.org/10.1523/JNEUROSCI.3061-17.2018

Mescher, M., Merkle, H., Kirsch, J., Garwood, M., & Gruetter, R. (1998). Simultaneousin vivo spectral editing and water suppression. *NMR in Biomedicine*, *11*(6), 266–272. https://doi.org/10.1002/(SICI)1099-1492(199810)11:6<266::AID-NBM530>3.0.CO;2-J

Mescher, M., Tannus, A., Johnson, M. O., & Garwood, M. (1996). Solvent Suppression Using Selective Echo Dephasing. *Journal of Magnetic Resonance, Series A*, *123*(2), 226–229. https://doi.org/10.1006/jmra.1996.0242

Meyerhoff, H. S., Papenmeier, F., & Huff, M. (2017). Studying visual attention using the multiple object tracking paradigm: A tutorial review. *Attention, Perception, & Psychophysics*, *79*(5), 1255–1274. https://doi.org/10.3758/s13414-017-1338-1

Mullins, P. G. (2018). Towards a theory of functional magnetic resonance spectroscopy (FMRS): A meta-analysis and discussion of using MRS to measure changes in neurotransmitters in real time. *Scandinavian Journal of Psychology*, *59*(1), 91–103. https://doi.org/10.1111/sjop.12411

Mullins, P. G. (2024). Considerations for event-related gamma-aminobutyric acid functional magnetic resonance spectroscopy. *NMR in Biomedicine*, *37*(11), e5215. https://doi.org/10.1002/nbm.5215

Mullins, P. G., McGonigle, D. J., O'Gorman, R. L., Puts, N. A. J., Vidyasagar, R., Evans, C. J., Cardiff Symposium on MRS of GABA, & Edden, R. A. E. (2014). Current practice in the use of MEGA-PRESS spectroscopy for the detection of GABA. *NeuroImage*, *86*, 43–52. https://doi.org/10.1016/j.neuroimage.2012.12.004

Nummenmaa, L., Oksama, L., Glerean, E., & Hyönä, J. (2017). Cortical Circuit for Binding Object Identity and Location During Multiple-Object Tracking. *Cerebral Cortex (New York, N.Y.: 1991)*, *27*(1), 162–172. https://doi.org/10.1093/cercor/bhw380

Ogg, R. J., Kingsley, P. B., & Taylor, J. S. (1994). WET, a T1- and B1-insensitive water-suppression method for in vivo localized 1H NMR spectroscopy. *Journal of Magnetic Resonance. Series B*, *104*(1), 1–10. https://doi.org/10.1006/jmrb.1994.1048

Okun, M., & Lampl, I. (2008). Instantaneous correlation of excitation and inhibition during ongoing and sensory-evoked activities. *Nature Neuroscience*, *11*(5), 535–537. https://doi.org/10.1038/nn.2105

Pelli, D. G. (1997). The VideoToolbox software for visual psychophysics: Transforming numbers into movies. *Spatial Vision*, *10*(4), 437–442. https://doi.org/10.1163/156856897X00366

Petroff, O. A. C. (2002). Book Review: GABA and Glutamate in the Human Brain. *The Neuroscientist*, *8*(6), 562–573. https://doi.org/10.1177/1073858402238515

Provencher, S. W. (1993). Estimation of metabolite concentrations from localized in vivo proton NMR spectra. *Magnetic Resonance in Medicine*, *30*(6), 672–679. https://doi.org/10.1002/mrm.1910300604

Provencher, S. W. (2001). Automatic quantitation of localized *in vivo* ^{1}H spectra with LCModel. *NMR in Biomedicine*, *14*(4), 260–264. https://doi.org/10.1002/nbm.698

Pylyshyn, Z. W., & Storm, R. W. (1988). Tracking multiple independent targets: Evidence for a parallel tracking mechanism*. *Spatial Vision*, *3*(3), 179–197. https://doi.org/10.1163/156856888X00122

Rademaker, R. L., Chunharas, C., & Serences, J. T. (2019). Coexisting representations of sensory and mnemonic information in human visual cortex. *Nature Neuroscience*, *22*(8), 1336–1344. https://doi.org/10.1038/s41593-019-0428-x

Schmidt-Wilcke, T., Fuchs, E., Funke, K., Vlachos, A., Müller-Dahlhaus, F., Puts, N. A. J., Harris, R. E., & Edden, R. A. E. (2018). GABA—from Inhibition to Cognition: Emerging Concepts. *The Neuroscientist*, *24*(5), 501–515. https://doi.org/10.1177/1073858417734530

Scholl, B. J. (2001). Objects and attention: The state of the art. *Cognition*, *80*(1–2), 1–46. https://doi.org/10.1016/S0010-0277(00)00152-9

Schuff, N., Meyerhoff, D. J., Mueller, S., Chao, L., Sacrey, D. T., Laxer, K., & Weiner, M. W. (2006). N-Acetylaspartate as a Marker of Neuronal Injury in Neurodegenerative Disease. In J. R. Moffett, S. B. Tieman, D. R. Weinberger, J. T. Coyle, & A. M. A. Namboodiri (Hrsg.), *N-Acetylaspartate* (Bd. 576, S. 241–262). Springer US. https://doi.org/10.1007/0-387-30172-0_17

Serences, J. T. (2016). Neural mechanisms of information storage in visual short-term memory. *Vision Research*, *128*, 53–67. https://doi.org/10.1016/j.visres.2016.09.010

Shibata, K., Sasaki, Y., Bang, J. W., Walsh, E. G., Machizawa, M. G., Tamaki, M., Chang, L.-H., & Watanabe, T. (2017). Overlearning hyperstabilizes a skill by rapidly making neurochemical processing inhibitory-dominant. *Nature Neuroscience*, *20*(3), 470–475. https://doi.org/10.1038/nn.4490

Shim, W. M., Alvarez, G. A., Vickery, T. J., & Jiang, Y. V. (2010). The Number of Attentional Foci and Their Precision Are Dissociated in the Posterior Parietal Cortex. *Cerebral Cortex*, *20*(6), 1341–1349. https://doi.org/10.1093/cercor/bhp197

Snyder, A. C., Morais, M. J., & Smith, M. A. (2016). Dynamics of excitatory and inhibitory networks are differentially altered by selective attention. *Journal of Neurophysiology*, *116*(4), 1807–1820. https://doi.org/10.1152/jn.00343.2016

Snyder, H. R., Hutchison, N., Nyhus, E., Curran, T., Banich, M. T., O'Reilly, R. C., & Munakata, Y. (2010). Neural inhibition enables selection during language processing. *Proceedings of the National Academy of Sciences*, *107*(38), 16483–16488. https://doi.org/10.1073/pnas.1002291107

Sprague, T. C., Ester, E. F., & Serences, J. T. (2014). Reconstructions of Information in Visual Spatial Working Memory Degrade with Memory Load. *Current Biology*, *24*(18), 2174–2180. https://doi.org/10.1016/j.cub.2014.07.066

Sprague, T. C., Saproo, S., & Serences, J. T. (2015). *Visual attention mitigates information loss in small- and large-scale neural codes*. *19*(4), 215–226.

Srivastava, S., Wang, W. Y., & Eckstein, M. P. (2023). *Bridging Neurons and Behavior in a Convolutional Neural Network with Emergent Human-like Covert Attention*. Neuroscience. https://doi.org/10.1101/2023.09.17.558171

Stagg, C. J. (2014). Magnetic Resonance Spectroscopy as a tool to study the role of GABA in motor-cortical plasticity. *NeuroImage*, *86*, 19–27. https://doi.org/10.1016/j.neuroimage.2013.01.009

Stanley, J. A., & Raz, N. (2018). Functional Magnetic Resonance Spectroscopy: The „New“ MRS for Cognitive Neuroscience and Psychiatry Research. *Frontiers in Psychiatry*, *9*, 76. https://doi.org/10.3389/fpsyt.2018.00076

Störmer, V. S., Alvarez, G. A., & Cavanagh, P. (2014). Within-Hemifield Competition in Early Visual Areas Limits the Ability to Track Multiple Objects with Attention. *The Journal of Neuroscience*, *34*(35), 11526–11533. https://doi.org/10.1523/JNEUROSCI.0980-14.2014

Störmer, V. S., Winther, G. N., Li, S.-C., & Andersen, S. K. (2013). Sustained Multifocal Attentional Enhancement of Stimulus Processing in Early Visual Areas Predicts Tracking Performance. *The Journal of Neuroscience*, *33*(12), 5346–5351. https://doi.org/10.1523/JNEUROSCI.4015-12.2013

Tamaki, M., Wang, Z., Barnes-Diana, T., Guo, D., Berard, A. V., Walsh, E., Watanabe, T., & Sasaki, Y. (2020). Complementary contributions of non-REM and REM sleep to visual learning. *Nature Neuroscience*, *23*(9), 1150–1156. https://doi.org/10.1038/s41593-020-0666-y

Townsend, J. T., & Ashby, F. G. (1978). Methods of modeling capacity in simple processing systems. In *Cognitive theory* (S. 199–239). Psychology Press.

Townsend, J. T., & Ashby, F. G. (viaf)94267600. (1983). *The stochastic modeling of elementary psychological processes*. Cambridge : Cambridge university press. http://lib.ugent.be/catalog/rug01:000725686

Tremblay, R., Lee, S., & Rudy, B. (2016). GABAergic Interneurons in the Neocortex: From Cellular Properties to Circuits. *Neuron*, *91*(2), 260–292. https://doi.org/10.1016/j.neuron.2016.06.033

Tritsch, N. X., Granger, A. J., & Sabatini, B. L. (2016). Mechanisms and functions of GABA co-release. *Nature Reviews Neuroscience*, *17*(3), 139–145. https://doi.org/10.1038/nrn.2015.21

Van Ede, F., & Nobre, A. C. (2023). Turning Attention Inside Out: How Working Memory Serves Behavior. *Annual Review of Psychology*, *74*(1), 137–165. https://doi.org/10.1146/annurev-psych-021422-041757

Van Essen, D. C. (2005). A Population-Average, Landmark- and Surface-based (PALS) atlas of human cerebral cortex. *NeuroImage*, *28*(3), 635–662. https://doi.org/10.1016/j.neuroimage.2005.06.058

Vaziri-Pashkam, M., & Xu, Y. (2017). Goal-Directed Visual Processing Differentially Impacts Human Ventral and Dorsal Visual Representations. *The Journal of Neuroscience: The Official Journal of the Society for Neuroscience*, *37*(36), 8767–8782. https://doi.org/10.1523/JNEUROSCI.3392-16.2017

Wehr, M., & Zador, A. M. (2003). Balanced inhibition underlies tuning and sharpens spike timing in auditory cortex. *Nature*, *426*(6965), 442–446. https://doi.org/10.1038/nature02116

Williams, S., Ralph, M. L., & Jung, J. (2023). *The role of GABA in semantic memory and its neuroplasticity*. https://doi.org/10.7554/eLife.91771.1

Wilson, M., Andronesi, O., Barker, P. B., Bartha, R., Bizzi, A., Bolan, P. J., Brindle, K. M., Choi, I.-Y., Cudalbu, C., Dydak, U., Emir, U. E., Gonzalez, R. G., Gruber, S., Gruetter, R., Gupta, R. K., Heerschap, A., Henning, A., Hetherington, H. P., Huppi, P. S., … Howe, F. A. (2019). Methodological consensus on clinical proton MRS of the brain: Review and recommendations. *Magnetic Resonance in Medicine*, *82*(2), 527–550. https://doi.org/10.1002/mrm.27742

Xu, Y. (2024). The human posterior parietal cortices orthogonalize the representation of different streams of information concurrently coded in visual working memory. *PLOS Biology*, *22*(11), e3002915. https://doi.org/10.1371/journal.pbio.3002915

Xu, Y., & Chun, M. M. (2009). Selecting and perceiving multiple visual objects. *Trends in Cognitive Sciences*, *13*(4), 167–174. https://doi.org/10.1016/j.tics.2009.01.008

Yamada, T., Watanabe, T., & Sasaki, Y. (2024). Plasticity–stability dynamics during post-training processing of learning. *Trends in Cognitive Sciences*, *28*(1), 72–83. https://doi.org/10.1016/j.tics.2023.09.002

Table 1. fMRS checklist proposed by Choi et al. (2021).

Site (Name or Number): Brain Imaging Center at University of Regensburg / Bezirksklinikum Regensburg 1. Hardware	
a. Field strength [T]	3 T
b. Manufacturer	Siemens
c. Model (software version if available)	Prisma
d. RF coils: nuclei (transmit/receive), number of channels, type, body part	64 channel head/neck coil
e. Additional hardware	N/A
2. Acquisition	
a. Pulse sequence	Siemens MEGAPRESS sequence; Siemens PRESS sequence
b. Volume of Interest (VOI) locations	Parietal lobe; occipital lobe
c. Nominal VOI size [cm^3, mm^3]	2 x 2 x 4 cm (parietal lobe); 2 x 2 x 2 cm (occipital lobe)
d. Repetition Time (TR), Echo Time (TE) [ms, s]	MEGAPRESS (Edit On & Edit Off): TR 1500 ms; TE = 68 ms; PRESS: TR 2000 ms; TE = 30 ms
e. Total number of Excitations or acquisitions per spectrum	MEGAPRESS: 472 scans in total, which corresponded to the following experimental conditions (summed across all time-points): on-ramp: 20 scans; cueing phase low load: 18 scans; tracking phase low load: 72 scans; response phase low load: 18 scans; cueing phase high load: 18 scans; tracking phase high load: 72 scans; response phase high load: 18 scans; intertrial interval 216 scans; off-ramp: 20 scans. For each participant all scans for the tracking phase of each load condition were averaged across trials with correct participant response. PRESS: 352 scans in total, which corresponded to the following experimental conditions (summed across all time-points): on-ramp: 32 scans; cueing phase low load: 9 scans; tracking phase low load: 54 scans; response phase low load: 9 scans; cueing phase high load: 9 scans; tracking phase high load: 54 scans; response phase high load: 9 scans; intertrial interval 144 scans; off-ramp: 32 scans. For each participant all scans for the tracking phase of each load condition were averaged across trials with correct participant response.

f. Additional sequence parameters (spectral width in Hz, number of spectral points, frequency offsets)	Spectral bandwidth: 1200 Hz; Spectral points: 1024
g. Water Suppression Method	WET
h. Shimming Method, reference peak, and thresholds for "acceptance of shim" chosen	Automated B_0 field mapping to < 20 Hz
i. Triggering or motion correction method	N/A
3. Data analysis methods and outputs	
a. Analysis software	LC Model Version 6.3-R; Osprey Version 2.4.0
b. Processing steps deviating from quoted reference or product	N/A
c. Output measure	Tissue-corrected concentrations relative to NAA from the same scan
d. Quantification references and assumptions, fitting model assumptions	Basis sets were imported from LC model software package and included the following spectra. MEGAPRESS difference: γ-Aminobutyric Acid (GABA), Glutamine (Gln), Glutamate (Glu), Glutathione (GSH), N-Acetylaspartate (NAA), N-Acetylaspartylglutamate (NAAG). PRESS: The basis set included spectra of Aspartate (Asp), Creatine (Cr), Phosphocreatine (PCr), γ-Aminobutyric Acid (GABA), Glucose (Glc), Glutamine (Gln), Glutamate (Glu), Glycerophosphocholine (GPC), Glutathione (GSH), myo-Inositol (Ins), L-Lactate (Lac), N-Acetylaspartate (NAA), N-Acetylaspartylglutamate (NAAG), scyllo-Inositol (Scyllo), Taurine (Tau).
4. Data Quality	
a. Reported variables	CRLB, shimming, S/N
b. Data exclusion criteria	CRLB > 25%, shimming >= 20 Hz, S/N < 5
c. Quality measures of postprocessing Model fitting	CRLB, NAA concentration in tracking phase with low and high load, S/N
d. Sample Spectrum	See Supplementary Figures 1 & 2

Figures

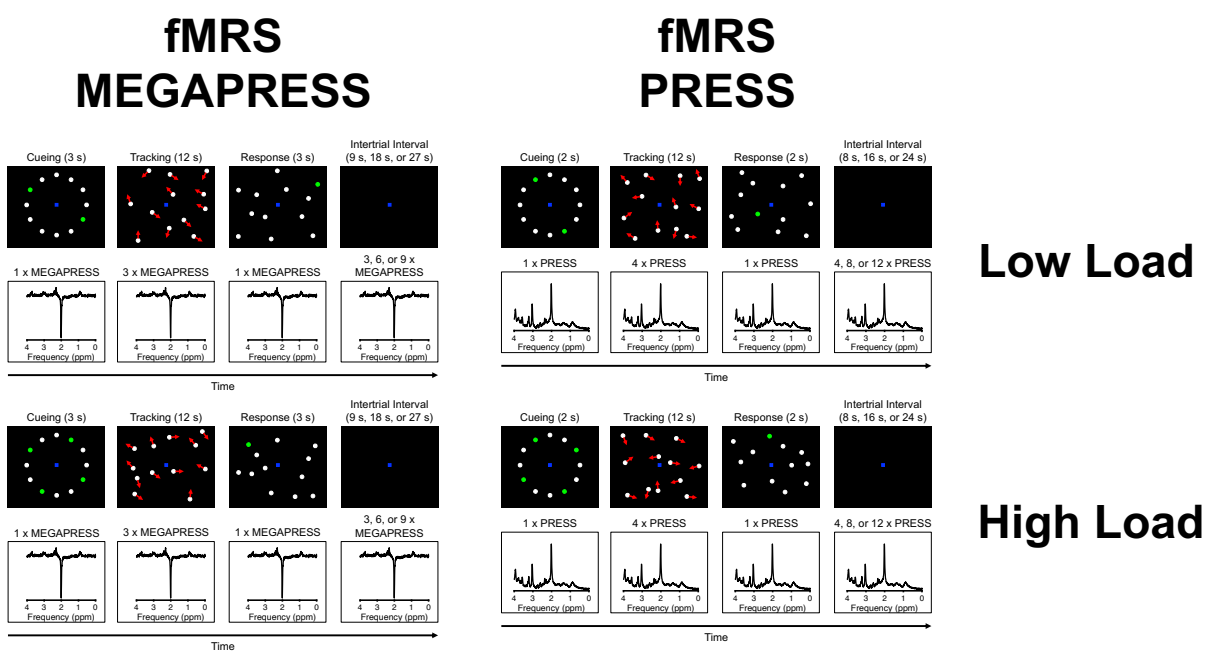

Figure 1. Example trials of the attentional tracking task with low and high load conditions in fMRS-MEGAPRESS and fMRS-PRESS.

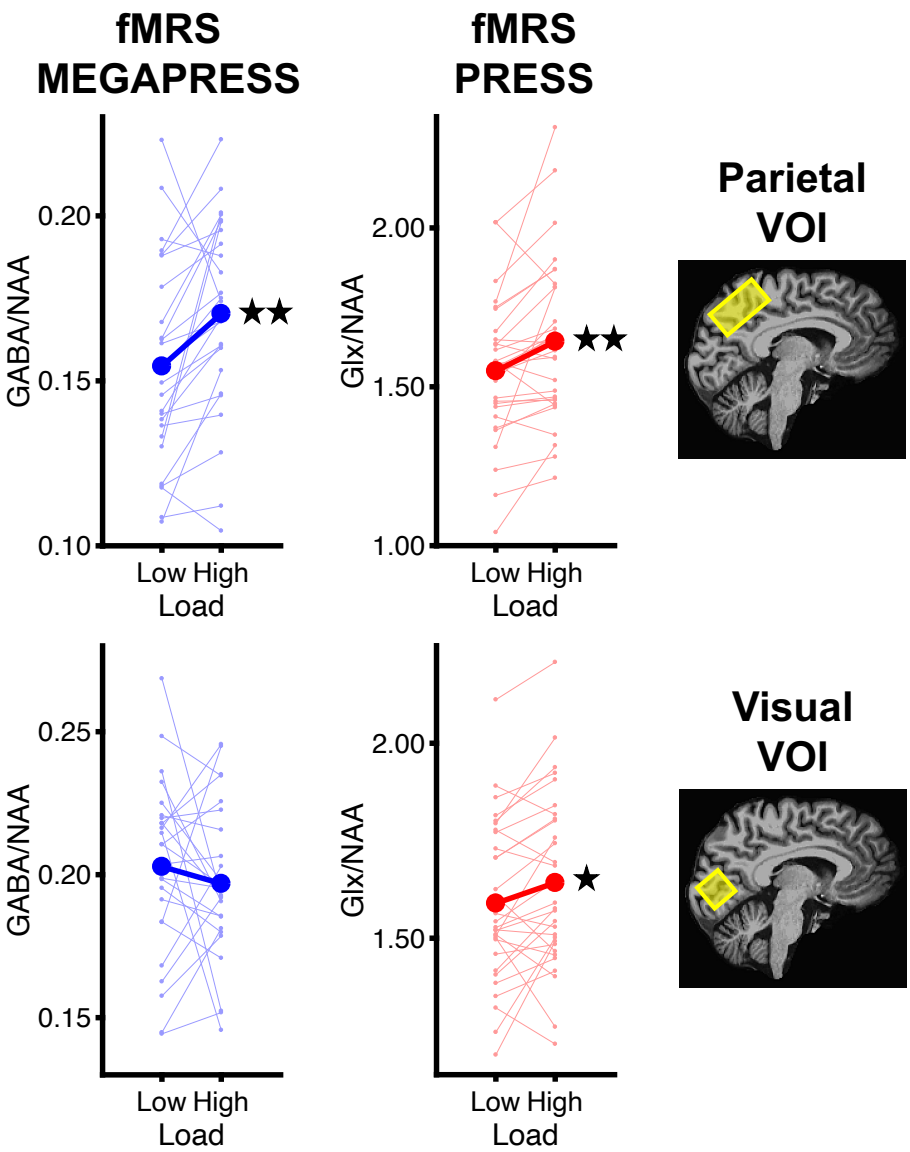

Figure 2. Load-dependent changes of metabolite concentrations in fMRS-MEGAPRESS and fMRS-PRESS. The thick line shows mean results across participants for the parietal and visual VOIs. Thin lines show results for each participant (26 participants for the parietal VOI in fMRS-MEGAPRESS, 25 participants for the visual VOI in fMRS-MEGAPRESS, 30 participants for each VOI in fMRS-PRESS). GABA = γ-aminobutyric acid. Glx = composite measure of glutamate and its precursor glutamine. NAA = N-acetyl-aspartate. Results of paired-sample *t*-tests between the low and high load conditions are denoted by asterisks: * $p < 0.05$, ** $p < 0.01$.

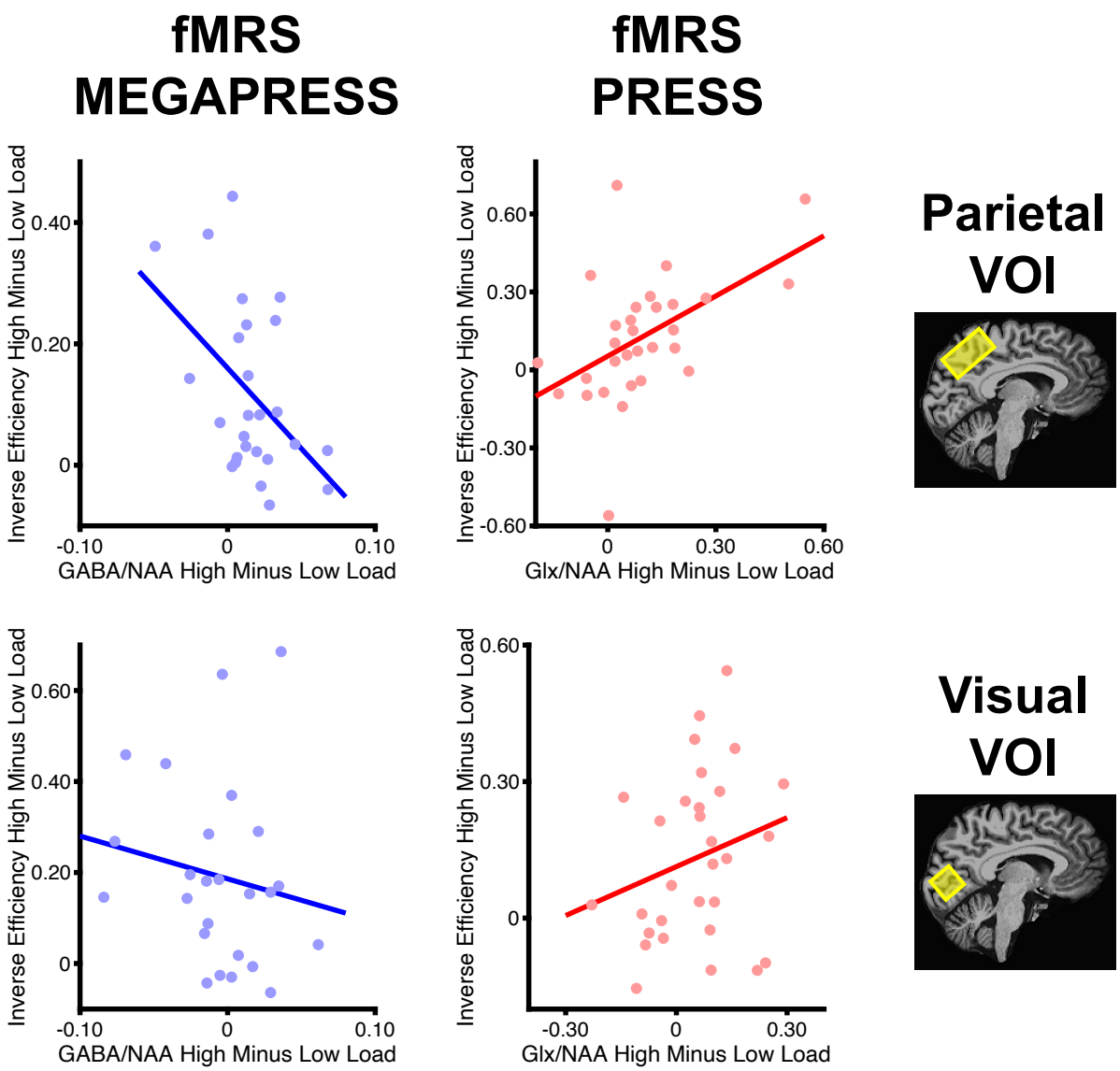

Figure 3. Correlation between load-dependent changes in metabolite concentrations and behavioral performance. Load-dependent changes in GABA and Glx were calculated by subtracting concentrations in low load from concentrations in high load for each participant. More positive values on the x-axis correspond to greater concentration increase from low to high load. Load-dependent changes in behavioral performance were calculated by subtracting the inverse efficiency score in low load from high load for each participant. More positive values on the y-axis correspond to greater increase of the inverse efficiency score from low to high load (i.e., greater decrease of response accuracy and greater increase of response time from low to high load). Each correlational analysis was carried out between metabolite concentrations and behavioral performance from the same fMRS run.

Supplementary Material

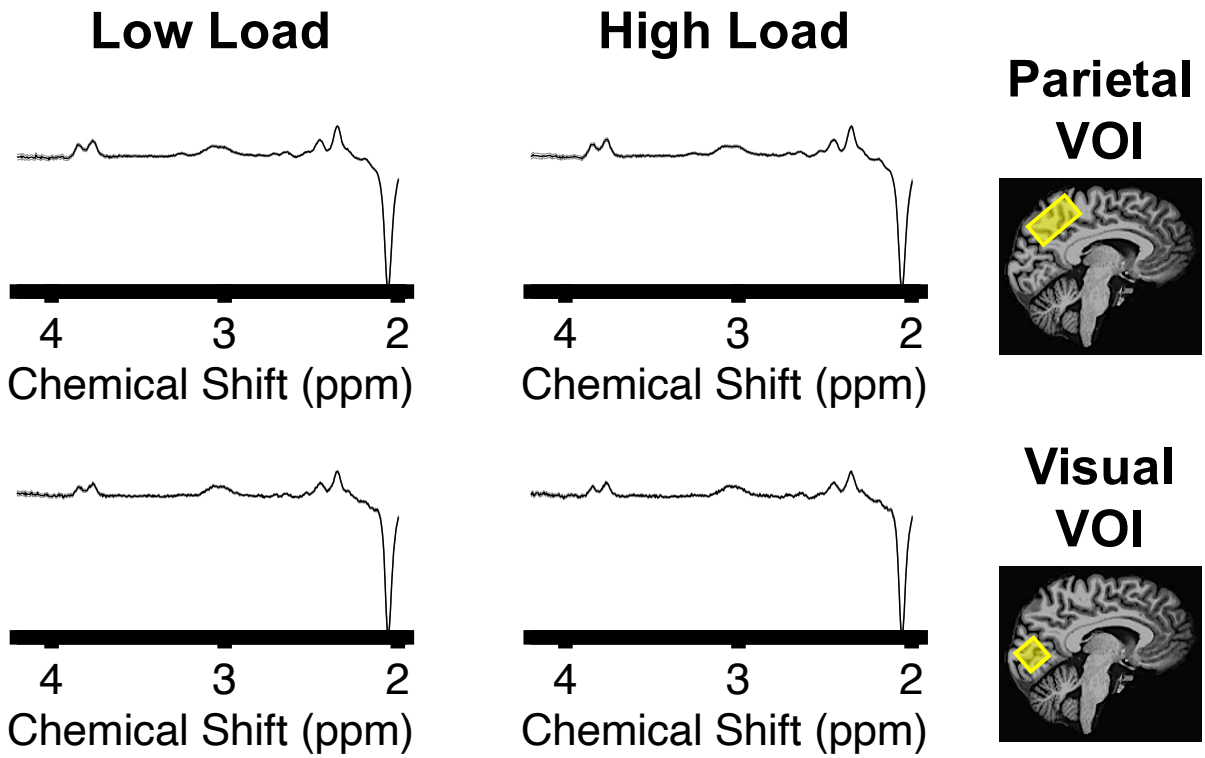

Supplementary Figure 1. Mean difference spectrum for each load condition and VOI in fMRS-MEGAPRESS across 26 participants (parietal VOI) and 25 participants (visual VOI). The gray shaded area shows standard-error-of-the mean. GABA at 3 ppm and NAA at 2 ppm.

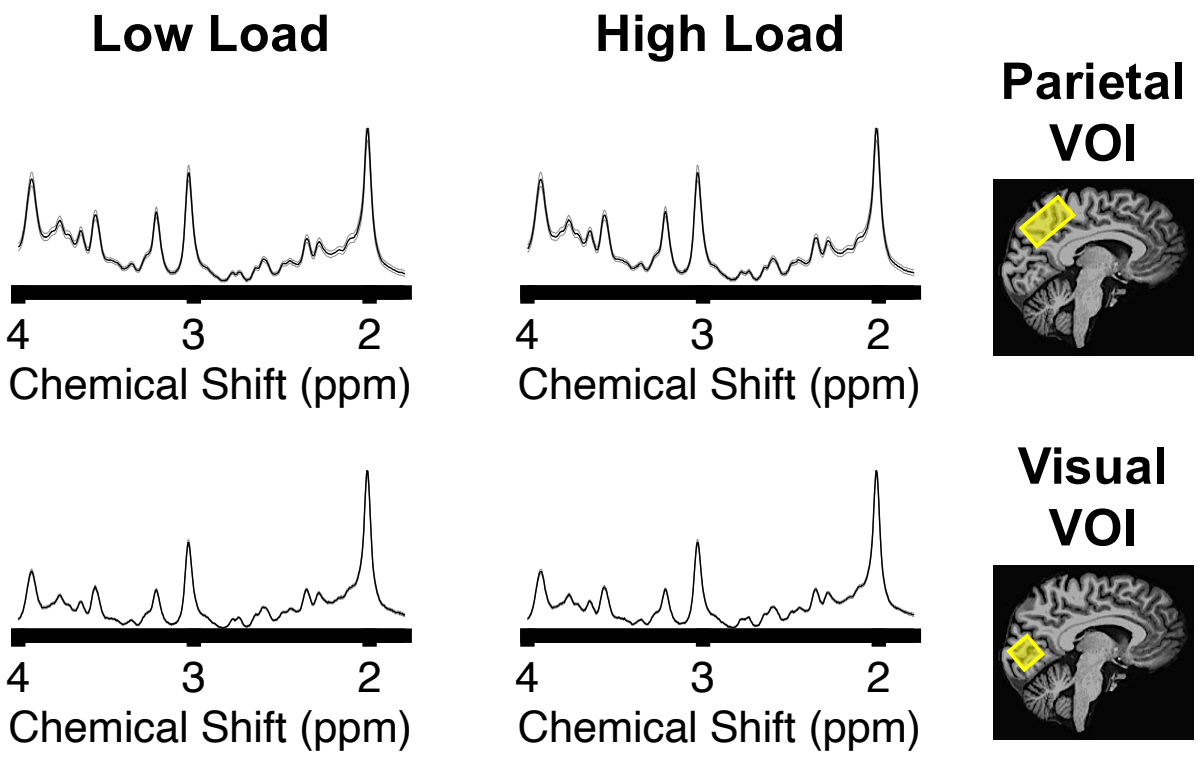

Supplementary Figure 2. Mean spectrum for each load condition and VOI in fMRS-PRESS across 30 participants. The gray shaded area shows standard-error-of-the mean. Glx between 2.1 and 2.5 ppm and NAA at 2 ppm.

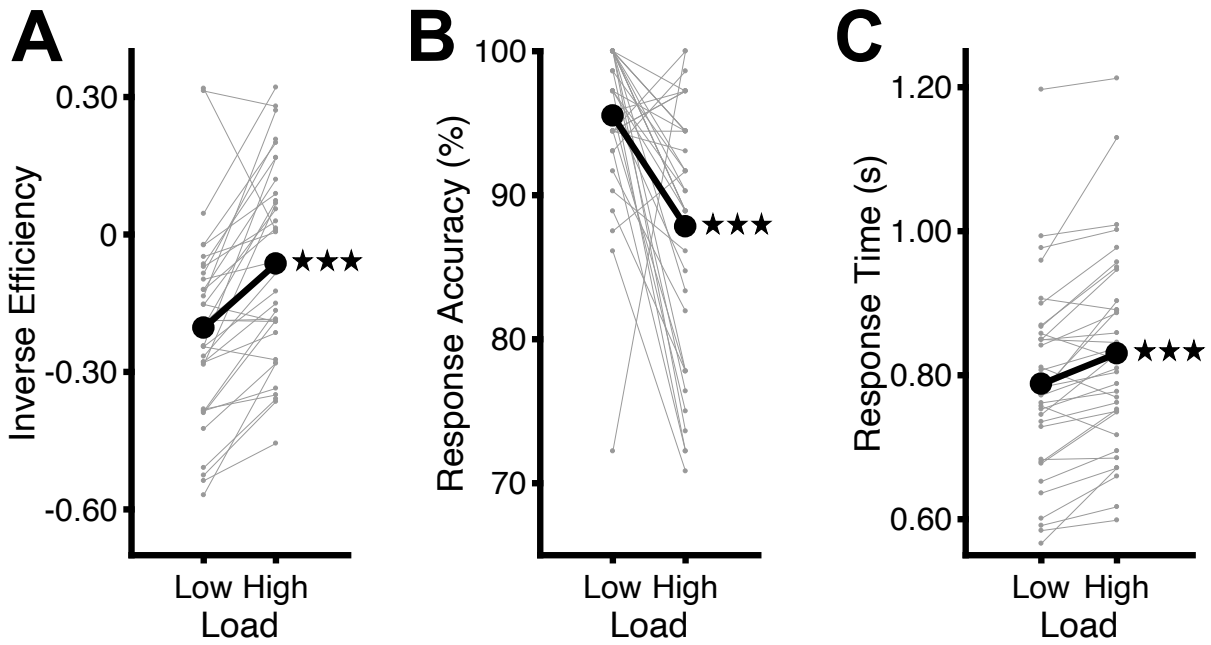

Supplementary Figure 3. Behavioral results across fMRS-MEGAPRESS and fMRS-PRESS. (**A**) Mean inverse efficiency score for each load condition across a total of 36 participants (thick line). Thin lines show results for each participant. The lower the score on the y-axis, the faster and more accurate participants responded. The result of a paired-sample *t*-test between the low and high load condition is denoted by asterisks: *** $p < 0.001$. (**B**) Results for response accuracy. Otherwise same as (A). The results of a paired-sample *t*-test on response accuracy (arcsin-square-root-transformed) showed a significant difference between high and low load conditions [$t(34) = -4.40$, $p < 0.001$, $d = -0.74$], suggesting that participants responded less accurately in the high than the low load condition. (**C**) Results for median response time. Otherwise same as (A). The results of a paired-sample *t*-test on response time (log-transformed) showed a significant difference between high and low load conditions [$t(34) = 5.42$, $p < 0.001$, $d = 0.92$], suggesting that participants responded slower in the high than the low load condition.

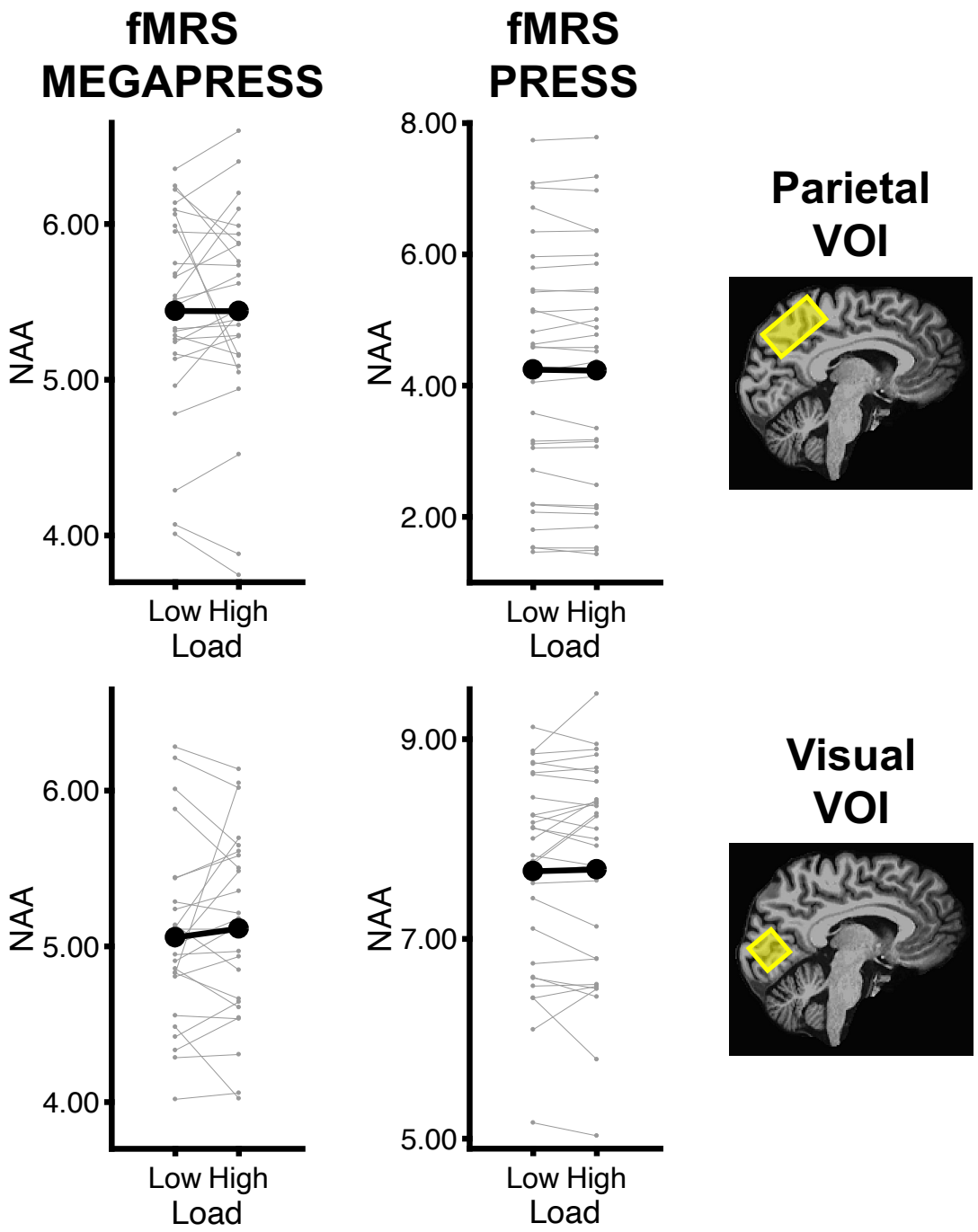

Supplementary Figure 4. Concentrations of the control metabolite N-acetyl-aspartate (NAA) in different load conditions of fMRS-MEGAPRESS and fMRS-PRESS. The thick line shows mean results across participants for the parietal and visual VOIs (26 participants for the parietal VOI in fMRS-MEGAPRESS, 25 participants for the visual VOI in fMRS-MEGAPRESS, 30 participants for each VOI in fMRS-PRESS). Thin lines show results for each participant.